# Experiment and Simulation of Heat Treatment Results of C-Ring Test Specimen

***Zhichao Li, B. Lynn Ferguson***
*Deformation Control Technology, Inc., Cleveland, Ohio, USA*

***Xichen Sun, Peter Bauerle***
*Materials Engineering, DaimlerChrysler Corporation, Detroit, MI, USA*

## Abstract

The C-Ring test specimen is regularly used to investigate the quality of heat treatment processes. In this study, C-Rings made of AISI 8620 steel were carburized, oil quenched, and tempered. A commercial heat treat simulation software package, DANTE®, was used to simulate the response of the C-Ring specimen to heat treatment. The model addressed furnace heating, carburization, transfer and immersion into the quench oil, and tempering. During quenching, the immersion direction was normal to the planar "C" shaped surfaces of the C-Ring, and the effect of immersion was found to be important to the final part shape. The thermal gradient between the top and bottom planes generated nonuniform distortion across the C-Ring opening in axial direction. The predicted results were validated by comparison against experimental measurements. The effect of different carburization schedules on the heat treatment response of the C-Ring in terms of dimensional change, phase and residual stress distributions are discussed in this study. Once validated, the simulation method provides a valuable tool that can be used in conjunction with selected experiments to cost effectively and accurately investigate the effects of alternative process routings on residual stress state and distortion.

## Introduction

Heat treatment is used to improve the quality and performance of steel components. A combination of austenizing, carburizing, quenching, and tempering processes normally generates compressive residual stress in the surface layer of the steel component, which is a key for improving fatigue life. However, distortion caused by heat treatment may increase the noise and reduce the fatigue life of gear components during service. It is both difficult and expensive to experimentally investigate the heat treatment process of a real part with complex geometry. The C-Ring shape has a changing cross-section thickness and it can be used to test the heat treatment process steps, including the process stability, cooling severity, and distortion. Heat treatment is a transient process, and the thermal gradient and phase transformations act together to cause distortion. In this paper, the complex process has been investigated by computer simulation using a commercial heat treat simulation package based on finite element method, DANTE®.[1] The kinetics models in DANTE effectively calculate the steel phase transformations during heating, quenching, and tempering process steps. The thermal gradient and phase transformations during heat treatment cause loading, unloading, and reverse loading at different locations of the component. The internal state variables implemented in DANTE addresses the above problem efficiently.[2, 3] In this study, DANTE is used to predict the heat treatment process of a C-Ring component. The effect of different carburization schedules on the amount of retained austenite, residual stresses, and distortion was predicted by the DANTE. Experiments were done by DaimlerChrysler, and the experimental results were used to compare the simulated results.

## Finite Element Model

Various C-Ring geometries have been used to characterize or as a witness of the heat treatment processes. The geometry of the C-Ring used for this study is shown in Figure 1(a). The OD and ID of the C-Ring are 50.8 *mm* and 31.7 *mm*, respectively. The center of the OD and ID has an offset of 6.35 *mm.* The height of the C-Ring is 19.05 *mm*, and the opening is 6.35 *mm.* The C-Ring has continuous wall thickness change from the opening to the back. The carbon profile, the variation in thermal gradient and the resultant timing differences in phase transformation affect the internal stress evolution during quenching, which generates a residual stress distribution in the different wall thickness locations of the C-Ring. The distortion at the opening of the C-Ring is magnified because of the geometrical effect. That is the main reason why C-Ring is used to characterize the quenching process.

Because the C-Ring geometry is symmetric, a half-symmetry finite element model was used for simulations. The finite

element mesh is shown in Figure 1(b), and it consists of 36,823 nodes and 33,110 quadrilateral elements. To simulate the carburizing process and capture the effect of carbon and thermal gradients in the shallow surface during quenching, four fine element layers were applied in the C-Ring exposed surface.

In this study, the C-Ring is made of AISI 8620 steel. The simulated heat treatment process includes furnace heating, carburization, air transfer from the furnace to oil tank, immersion and holding the part in agitated quench oil, air cooling to ambient, and low temperature tempering. The half symmetric model can capture the effect of immersing the C-Ring in a direction either vertical to the flat "C-shaped" surface or parallel to the symmetric surface. In this paper, only the immersion direction vertical to the flat "C-shaped" surface was considered.

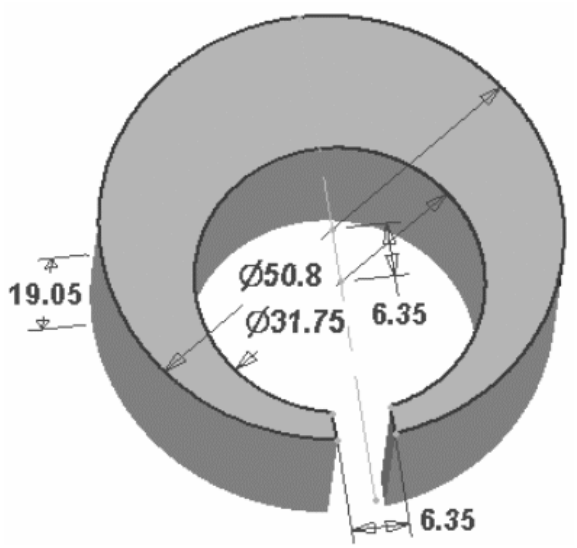


*(a)*

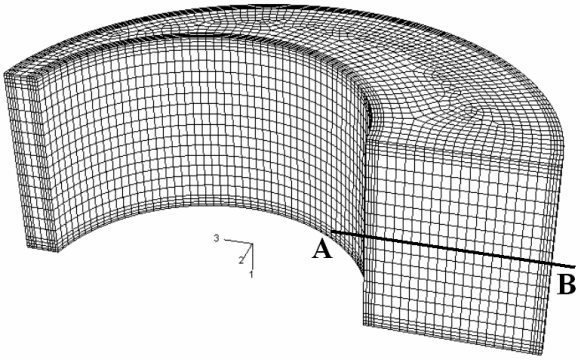


*(b)*

*Figure 1: (a) C-Ring Geometry (unit: mm) (b) Finite Element Meshing.*

**Phase Transformation Kinetics and Mechanical Models**

Phase transformation models for a steel heat treatment process must include kinetics for heating, cooling, and tempering. The heating models include austenite formation from ferrite, pearlite, bainite or martensite. The possible cooling models include austenite decomposing to ferrite, pearlite, bainite or martensite. In this case, the tempering model covers the transformation of as-quenched martensite to tempered martensite. Kinetics indicates that the models cover the rates of these transformations.

The diffusive phase transformation model parameters in the DANTE database include ferrite, pearlite, upper bainite, and lower bainite formation on cooling and austenite formation on heating. Upper bainite and lower bainite are treated as two separated phases because they have significant strength differences based on the formation temperature.[4] Equation (1) is the general form of the cooling kinetics model for diffusive transformations.

$$\frac{d\phi_d}{dt} = \nu_d(C,T)\cdot \phi_d^{\alpha_d}\cdot \phi_a^{\beta_d} \qquad (1)$$

where $\phi_d$ is the volume fraction of the diffusive phases; $\phi_a$ is the available volume fraction of austenite; $t$ is the transformation time; $T$ is temperature; $C$ is carbon content; $\nu_d$ is the transformation mobility, with $\nu_d$ being a function of temperature and carbon; and the exponents $\alpha_d$ and $\beta_d$ are phase dependent constants.

Different from the diffusive transformations, the martensitic phase transformation is temperature driven, as shown in equation (2).

$$\frac{d\phi_m}{dT} = -\nu_m(C,T)\cdot \phi_m^{\alpha_m}\cdot \phi_a^{\beta_m} \qquad (2)$$

where $\phi_m$ is the volume fraction of martensite; $\phi_a$ is the available volume fraction of austenite; $T$ is temperature; $C$ is carbon content; $\nu_m$ is the mobility of martensitic transformation; and $\alpha_m$ and $\beta_m$ are constants.

The DANTE package includes a set of utility programs used to fit the kinetics parameters required for the FE heat treatment simulations. Sources of data used for fitting the kinetics parameters include dilatometry, published isothermal transformation (TTT) and continuous cooling transformation (CCT) diagrams, and Jominy end-quench data. Among all the available kinetics characterization data, dilatometry data provides the best accuracy because it includes all the necessary time-temperature-strain data.[5] However, the dilatometry data is often not available, and I tmay not be feasible to run experiments. In place of dialtometry data, available TTT/CCT diagrams may be used to determine the kinetics equation parameters. Note that transformation strain values must be estimated with this method. DANTE has

utilities to then generate TTT and CCT diagrams, and Jominy curves using the fitted kinetics parameters. These curves can be compared with availabe handbook or other experimental data to assess parameter accuracy.

The Bammann-Chiesa-Johnson (BCJ) internal state variable mechanical model is used in DANTE to describe the material reponse driven by thermal gradient and phase transfromations during heat treatment.[2, 3] Instead of using effective strain as the material state variable, the BCJ model uses a tensor variable to describe the material condition. Furthermore, the BCJ model can accomodate the loading and unloading processes happening due to the thermal gradients and phase transformations that occur during heat treatment of steels.

**Heat Treatment Process Description**

The heat treatment process in this study included furnace heat up, gas carburization, air transfer from the furnace to quench tank, immersion and holding in quench oil, air cooling to room temperature, and tempering. The two carburization schedules investigated were:

- Schedule 1: carburization at 925º C for 6 hours at an atmosphere carbon potential of 0.9%.
- Schedule 2: carburization at 925º C for 6 hours at an atmosphere carbon potential of 1.1%.

The air transfer between the furnace and quench tank took 10 seconds. The C-Ring was immersed into the oil tank at a speed of 40 *mm/sec* in the direction vertical to the "C-shaped" flat surface. The height of the C-Ring in the axial direction was 19.05 *mm*, so part immersion into the agitated oil took 0.5 seconds. After immersion, the C-Ring was held in the 65º C oil for 10 minutes. After holding in the oil, the C-Ring was taken out and air cooled to room temperature. The C-Ring was then tempered at 150º C for 2 hours.

The AISI 8620 data available in DANTE database was used for these simulations, and the data include:

- Carbon diffusion properties at different temperatures;
- Heat transfer coefficients during furance heating, and oil quenching;
- Phase transformation kinetics data as a function of carbon level;
- Thermal properties in terms of temperature and carbon for individual phases; and
- Mechanical properties in terms of temperature and carbon for individual phases.

**Results and Discussions**

DANTE uses a mass diffusion model to simulate the carburization process. The exterior C-Ring surfaces were exposed in the carbon atmosphere during carburization. The final internal carbon distributions for the two carburization schedules are shown in Figure 2 for quarter C-Ring sections.

Figure 2 shows the carbon distribution profile along the cut faces. The wall thickness of the C-Ring increases continuously from the opening to the back. Therefore, the ratio of the carbon case depth to the wall thickness decreases from the opening to the back. As a result, the average carbon content at the thin opening is higher than the thick back section. The surface carbon at the ring corners is higher than the carbon in the center of a planar face, and the carbon the OD curved surface is slightly higher than the carbon in the curved ID surface.

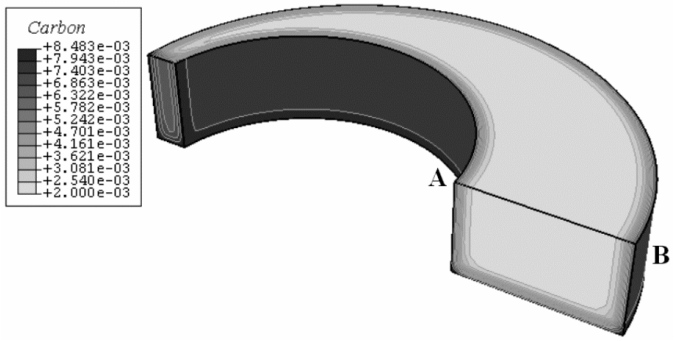


*(a)*

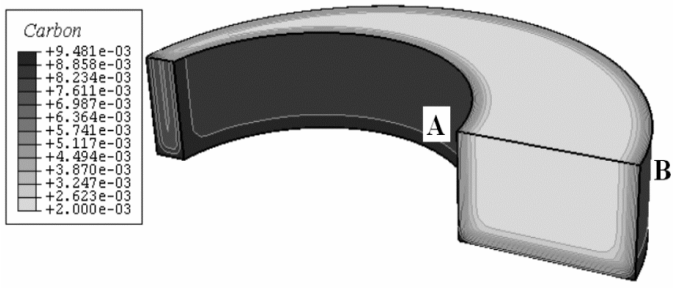


*(b)*

*Figure 2: Carbon Distribution Profile: (a) Carburization Schedule 1, (b) Carburization Schedule 2.*

The carbon distribution along the line AB in Figure 2 is shown in Figure 3. The X-axis is the depth from either ID or OD surfaces along the line AB. The Y-axis is the carbon content. From Figure 3, carburization schedule 1 (CP of 0.9%C) predicted a final carbon content at the ID surface of 0.78%. The experimental result was 0.77%. For carburization schedule 2 (CP of 1.1%C), the predicted carbon content at the ID surface is 0.89%, and the experimental result was 0.87%. For both schedules, the carbon content at the OD is slightly higher than the ID carbon content due to the geometry effect of the surface curvature. Using 0.5%C to define case depth, the predicted case depths for these two schedules were 0.7 *mm* and 0.8 *mm*, respectively.

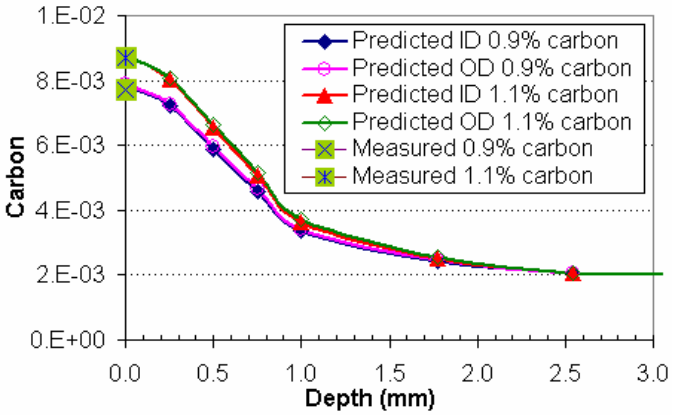


*Figure 3: Carbon Distribution along Line AB (Figure 2).*

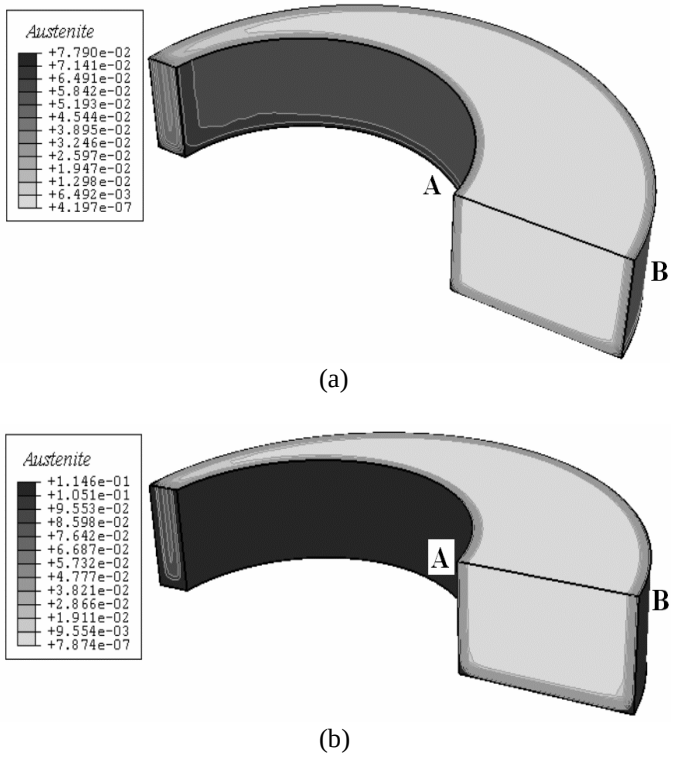


*Figure 4: Retained Austenite Distribution Contour: (a) Carburization Schedule 1, (b) Carburization Schedule 2.*

After heat treatment, any retained austenite may decompose continuouly during the service. The small, localized volume increase caused by the newly formed phase may increase the noise of a gear component. Therefore, the volume fraction of retained austenite after heat treatment is very important. For the same steel grade, the higher carbon content of the case depresses the martensitic transformation starting temperature, and, as a result, the volume fraction of retained austenite increases with the carbon level. Figure 4 shows the predicted contours of retained austenite after quenching for both carburization schedules. There is about 7% retained austenite at the carburized surface predicted for schedule 1, and there is no retained austenite predicted in the C-Ring core where the base carbon level exists. Figure 4(b) shows that the predicted amount of retained austenite for carburization schedule 2 in the case is about 11%, since the higher carbon content further depresses the martensitic transformation starting temperature. In the C-Ring core, there is no retained austenite predicted for schedule 2, just as none was predicted for schedule 1.

No ferrite and pearlite were predicted after quenching for both carburization schedules. The main phases after quenching were lower bainite and martensite. Figure 5(a) shows the lower bainite distribution after oil quenching and air cooling to ambient for rings processed using carburization schedule 1 (0.9% CP). A volume fraction of about 45% lower bainite was predicted in the center of the thickest cross section; rings processed using schedule 2 (1.1% CP) had a similar lower bainite distribution. The predicted volume fraction of upper bainite has a maximum value of 5% at the center of the thickest cross section. Figure 5(b) shows the predicted martensite distribution for rings processed using carburization schedule 1. The thin cross section has about 95% martensite. The volume fraction of martensite at the surface is slightly lower than a shallow depth location because of the retained austenite caused by higher carbon content. The lowest martensite volume fraction, 45%, is in the center of the thickest cross section.

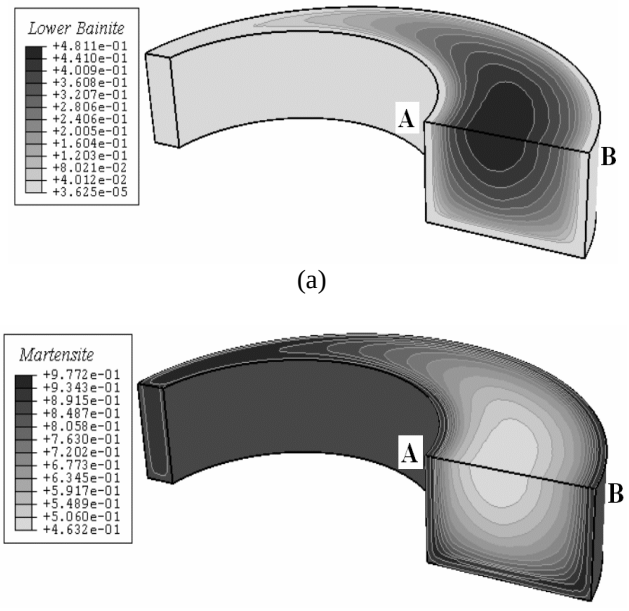


*Figure 5: Phase Distribution Contours: (a) Lower Bainite, (b) Martensite for C-Rings Processed Using Schedule 1.*

Figure 6 shows the phase distributions along line AB. The X-axis is the length from point A to point B. The points X=0 *mm* and X=15.875 *mm* stand for the surface points A and B, respectively. The curves with the square marks are the retained austenite distributions after quenching using both

carburization schedules. As mentioned, the retained austenite at the surface is about 11% for schedule 2 rings and 7% for schedule 1 rings. The core location of the C-Ring has a base carbon content of 0.2%, and there is no retained austenite predicted at the core location after oil quenching and air cooling. The curves with the circle marks are the bainite distributions along line AB. There is no bainite predicted right on the surface because the cooling rate at the surface is fast and the high carbon delays bainite transformation. About 50% bainite (lower plus upper bainite) is predicted at the center of the thickest cross section as shown in Figure 6 at a location with X=9 *mm*. At a depth of 1.5 *mm* from either ID or OD surfaces, the volume fraction of bainite from the carburization schedule 1 is slightly higher than that from the carburization schedule 2, which is caused by a combined effect of the cooling rate and the carbon content effect on transformation kinetics.

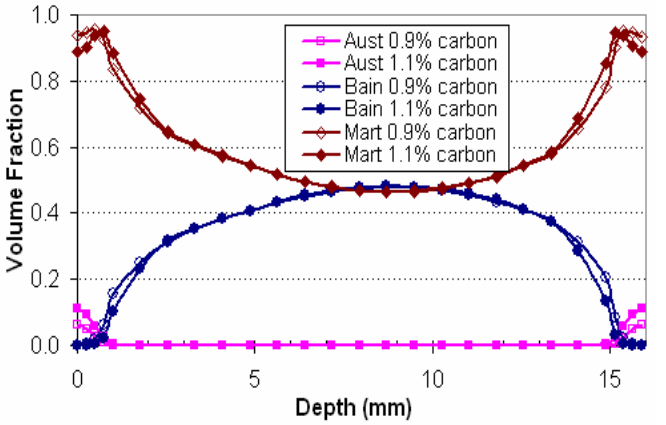


*Figure 6: Volume Fractions of Different Phases of As-Quenched Condition along Line AB (Figure 2).*

At the same depths from both ID and OD surfaces, the volume fractions of bainite are less from the ID surface side than from the OD surface, which is purely due to the ID-OD differences of the carbon profiles. The surface area to the mass ratio of the ID location is less than that of the OD location. As a result, the cooling rate immediately below the ID surface is lower than the cooling rate immediately below the OD surface at the beginning of the quenching process. After a certain time period of holding the part in the quench tank, the cooling rate inside the ID surface catches up and exceeds the cooling rate inside the OD surface. Over the entire quenching period, the location inside the OD surface stays in the bainite transformation temperature region longer than the location inside the ID surface, which causes a slightly higher bainite volume fraction closer to the OD surface than the ID surface. At locations below the carburized case, the austenite that doew not transform to bainite will transform to martensite, so the martensite in the C-Ring core has an opposite distribution profile to the bainite, as shown in Figure 6, i.e. there is slightly higher martensite content toward the ID of the ring than toward the OD.

The hardness distribution is used in industry to check the quenching results. Figure 7 shows the comparisons between the measured hardness and the predicted hardness. Hardness calculations in DANTE simulations are based on the volume fractions of phases, the temperatures of phase formation, and carbon content. Figure 7(a) and Figure 7(b) are the hardness distributions after tempering using both carburization schedules, respectively. At a depth less than 0.5 *mm* from the surface, the main phase is martensite, as shown in Figure 6. The hardness decrease from the surface to a depth of 0.5 *mm* is small. At depths greater than 0.5 mm, the volume fraction of bainite increases rapidly, hardness decreases rapidly because of the decrease of martensite volume fraction and carbon content. The surface hardness using the carburization schedule 2 is 65 HRC, and the surface hardness using the carburization schedule 1 is 63.5 HRC. The core hardness is the same for the two carburization schedules, just as the microstructures are predicted to be similar.

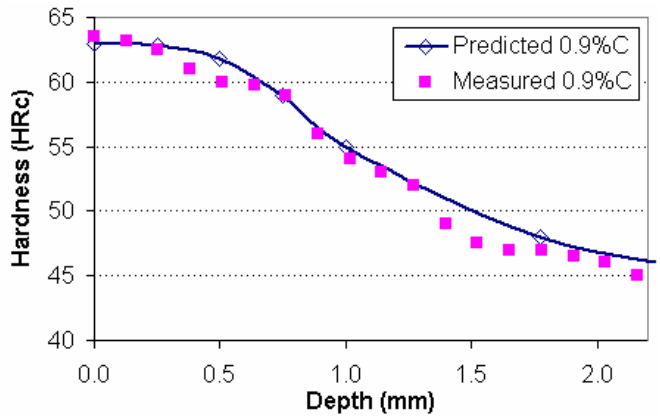


(a)

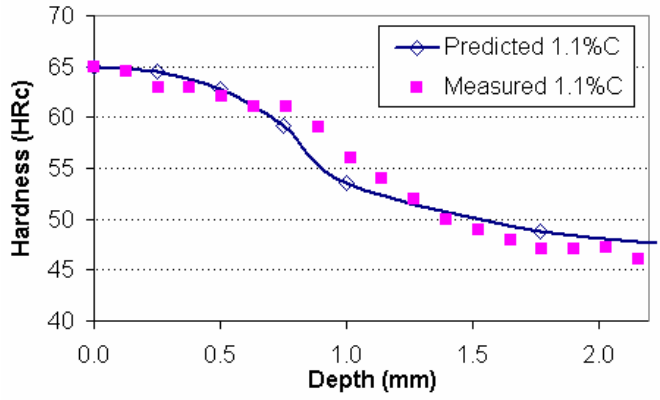


(b)

Figure 7: Hardness Distributions*: (a) Carburization Schedule 1, (b) Carburization Schedule 2.*

Due to the unbalanced geometry of the C-Ring, changes in the distance across the "C" opening caused by heat treatment are magnified. The predicted opening displacements of both the ID and OD edges at different heat treatment stages are plotted in Figure 8. The opening displacement is defined as the

distance change between either the two ID edges or the two OD edges. The X-axis in Figure 8 is the height in *mm* along the axial direction with the X=0 *mm* being immersed into the oil tank first. The Y-axis is the opening displacement in *mm*. In Figure 8, a zero opening displacement means that there is no distance change between the two edges, and a positive opening displacement means the distance between the two edges increases.

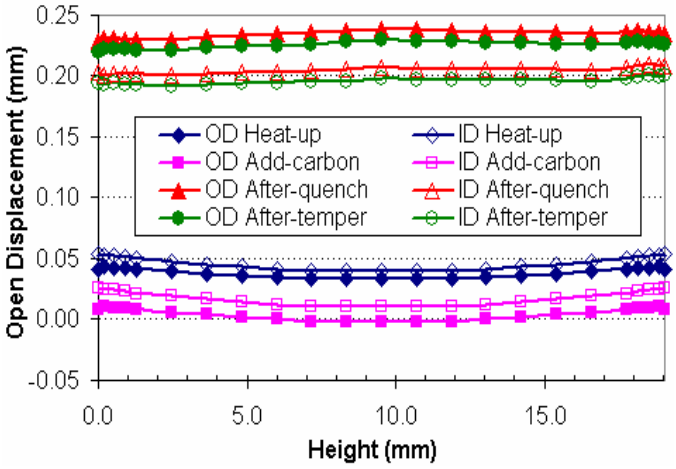


(a)

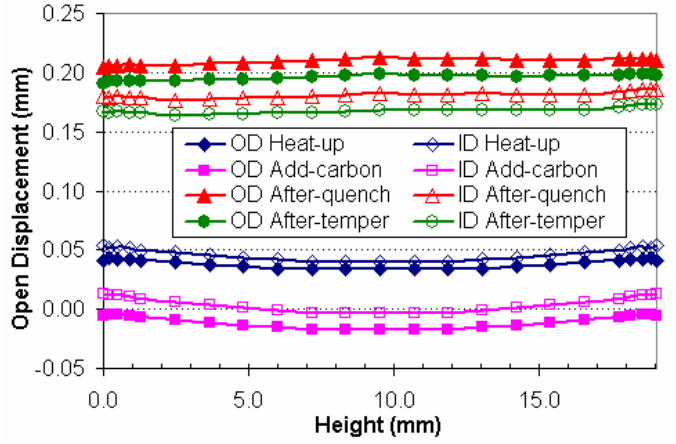


(b)

*Figure 8: "C" Opening Displacements at Different Heat Treatment Stages: (a) Carburization Schedule 1, (b) Carburization Schedule 2.*

The nonuniform temperature distribution between the thin and thick cross sections during heating causes nonuniform austenite formation during heating. The combined effect of both thermal gradient and nonuniform austenite formation generated distortion during heating, as shown by the curves with diamond marks in Figure 8. The curves with the solid and hollow diamond marks are the OD opening and ID opening displacements right after heating up, respectively. As shown in Figure 8, the opening after heating was increased, with the OD displacement being slightly less than the ID displacement. This distortion was due to the combination of thermal expansion and the temporary contraction due to austenite formation. The opening displacement due to pure thermal expansion calculated by using the CTE and original open distance is about 0.0001 *mm*. The predicted opening displacement by DANTE after heating up is about 0.05 *mm*, which is much larger than 0.0001 *mm*. Therefore, the main distortion generated during heat up is shape change instead of pure size change. The nonuniform thermal profile and austenization transformations are the main cause of the distortion during heating. The opening displacement after heating shows a bowing distortion with a smaller opening at the middle height location.

With the addition of carbon, the opening displacements of both the ID and OD edges were reduced, as shown by the curves with the square marks. However, both the bowing distortion and the difference between the OD opening and ID opening were increased. In Figure 8, the differences between the curves with the diamond marks and the curves with the square marks are the pure distortion caused by carburization. With higher atmosphere carbon content, the distortion caused by carburization is larger, which is shown by the difference between Figure 8(a) and Figure 8(b).

After carburization, the C-Ring was transferred from the furnace to the quench tank in 10 seconds, and then immersed into the quench tank with the immersion direction vertical to the planar "C-shaped" surface. The opening displacements after quenching are shown as the curves with the triangle marks. The difference between the ID opening and the OD opening is about 0.04 *mm* for both carburization schedules. The opening displacement after quenching using the carburization schedule 2 is about 0.025 *mm* less than that of carburization schedule 1. The effect of immersion is shown by the difference of the opening displacements at the bottom and the top of the edges, as shown in Figure 8. After tempering, the "C" opening was reduced by about 0.01 *mm* from the quenched and air cooled position, as shown by the curves with circle marks. The final "C" opening position is wider than the initial green position, with the OD displaced more than the ID edge; this means that the ring grew but more importantly that the "C" distorted.

The opening displacement after heat treatment for C-Rings processed using carburization schedule 1 is greater than that for C-Rings processed using carburization schedule 2, c.f. 0.22 mm vs. 0.18 mm. The DANTE simulations show that the opening distortion during heat treatment changes significantly due to the thermal gradient and sequence of phase transformations. The opening displacement is very sensitive to the heat treatment process, such as carburization schedules, cooling rate, and tempering temperature. Therefore, the C-Ring can be used to check the heat treat process stability.

The residual stress distribution after heat treatment is very important to fatigue life, with compressive residual stress in the carburized case improving fatigue life. Figure 9 shows the

minimum principal stress distribution contours after the heat treatment for both carburization schedules.

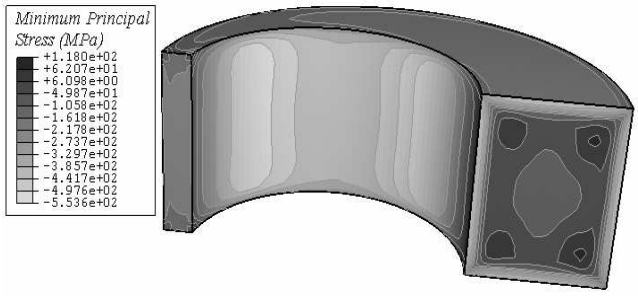


(a)

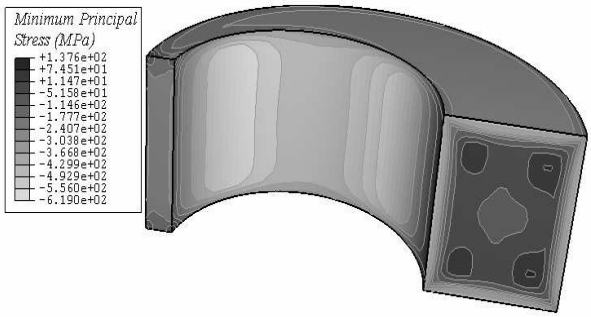


(b)

*Figure 9: Residual Stress Distributions: (a) Carburization Schedule 1, (b) Carburization Schedule 2.*

The compressive residual stresses along both ID and OD surfaces show a wave shape in the circumferential direction, which is caused by the geometrical effect. Higher surface carbon generates higher surface compression that extends deeper into the part, which is shown by the visual difference between Figures 9(a) and 9(b). By increasing the atmosphere carbon content from 0.9% to 1.1% during carburization, the predicted minimum pincipal stress on the surface increased about 50 MPa in magnitude. The residual stress on the ID surface is about 60 MPa higher in compression than the residual stress on the OD surface. The core of the C-Ring is shown to be under tensile to balance the residual surface compression.

The residual hoop stress was measured to verify the simulations. In Figure 10, the X-axis is the depth in *mm* from the OD surface along the line AB (Figure 2), and the Y-axis is the residual hoop stress in MPa. The solid lines are the predictions using DANTE, and the circle points are the measurements using X-ray method.

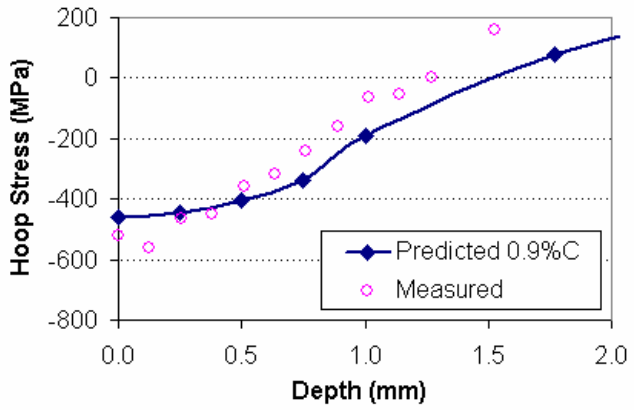


(a)

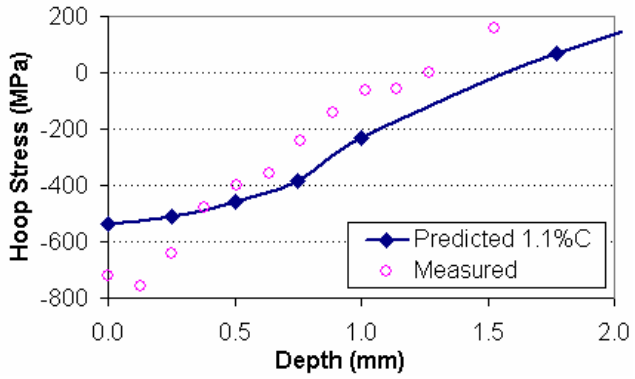


(b)

*Figure 10: Residual Stress Distributions: (a) Carburization Schedule 1, (b) Carburization Schedule 2.*

## Conclusions

The heat treatment processes of a C-Ring with nonuniform wall thickness were simulated using DANTE, a commercial heat treatment simulation software package. Two gas furnace carburization schedules were simulated. The effect of different carburization schedules on the phase distribution, residual stress distribution, and distortion was predicted and discussed. The hardness and residual stress distributions were validated by experiments. Due to the C-Ring's geometry, the residual stress distributions on both the ID and OD surfaces in the circumferential direction are nonuniform, and the residual stress on the ID surface is higher in compression than the stress on the OD surface. Higher carbon content in the carburized case tends to generate higher compressive residual stress in the surface. The simulation and experimental results show that the nonuniform C-Ring's opening displacement is very sensitive to the heat treatment process, such as carburization schedule, heating and cooling rate, and tempering. The C-Ring can be used as a witness during the heat treatment process to check the process quality and stability.

## References


1. B. Lynn Ferguson, A. Freborg, and G. Petrus, "Software Simulates Quenching", *Advanced Materials and Processes*, H31-H36, August (2000)
2. D. J. Bammann et al, *Modeling A high Temperature Forging of 304L Stainless Steel*, NUMIFORM'95: The Fifth International Conference on Numerical Methods in Industrial Forming Processes, Ithaca New York 1995, 215-218
3. D. J. Bammann and A. R. Ortega, The Influence of the Bauschinger Effect and Yield Definition on the Modeling of Welding Processes, Welding and Advanced Solidification Processes-VI. Warrendale, PA: The minerals, Metals & materials Society, 1993, 543-551
4. F. B. Pickering, "The structure and properties of bainite in Steels", Transformation and Hardenability in Steels, February 27-28, 1967 109-129
5. Z. Li, B. Lynn Ferguson, and A. M. Freborg, "*Data Needs for Modeling Heat Treatment of Steel Parts*", Proceedings of Materials Science & Technology Conference, 219-226, September (2004)